A fluorescence spectrum of molecular oxygen

H.S. Nieman
(Dated: August 26, 2008)

A theoretical study has been performed to assign an experimental fluorescence spectrum of molecular oxygen. This spectrum is observed upon multi-photon absorption of 193.4 nm light and has the property that it consists of distinct discrete and continuum parts. The final state of the fluorescence process in the discrete part of the spectrum has been determined by calculating the energy of its dissociation limit. The approximate energy of the separation between the discrete and continuum parts of the spectrum and the known photon excitation energy have been used to do this. It turned out that the final state is $O_2B^3\Sigma_u^-$. The intermediate state is a Rydberg state with an $O_2^+a^4\Pi_u$ core, which is determined by using molecular orbital diagrams and electron spin conservation. By combining an RKR method with a sinc-DVR method, relative intensities for peaks in the discrete part of the spectrum have been calculated for different vibrational levels of the intermediate state. From these simulated spectra, it has been determined that the intermediate state is likely to be a $\nu' = 11$ vibrational level with a quantum defect of $\delta = 1.281$.

I. INTRODUCTION

Molecular oxygen, O_2, is undoubtedly one of the best investigated molecules on earth, in terms of spectroscopy as well, since it has importance both in atmospheric science and in combustion processes. An extensive review of the spectroscopy of the neutral O_2 and singly ionized O_2^+ molecule was published in 1972 [1] and many new data have been added since. It would therefore come as a surprise to find features in absorption or emission spectra of O_2 that do not belong to any known transition. Nonetheless, that is exactly the topic of this study, a part of the emission spectrum of molecular oxygen that has resisted assignment up to now, even though it has been reported several times during the past 20 years. The spectrum, shown in figures 1 and 2, was discovered (or rediscovered, as it turned out later) serendipitously in the laboratory of the Applied Molecular Physics department in Nijmegen during research into the chemistry involved in the production of NO that occurs when an ArF laser beam is tightly focused in air. (J. Bominaar & N. Dam, personal communication) It is only observed when the laser beam is focused, which indicates that a multi-photon absorption is involved. The spectrum is cut off at 195 nm, since glass becomes intransparant at this wavelength. The energy state from which the multi-photon absorption takes place is the vibronic ground-state $X^3\Sigma_g^-(\nu = 0)$ of neutral oxygen, O_2. Potential energy curves of neutral oxygen and of the oxygen ion that are relevant for this problem are drawn in figure 3. Both the upper and lower vibronic states of the emission (fluorescence) are unknown.

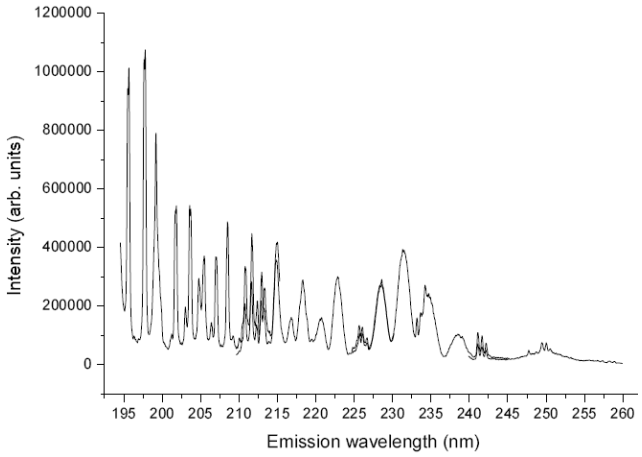

Figure 1: The observed fluorescence spectrum of pure molecular oxygen at "zero pressure" as it has been measured by N.Dam ea.

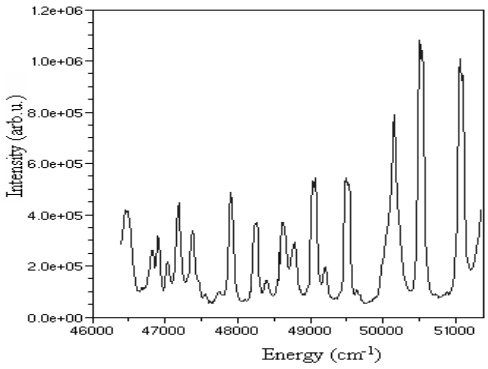

Figure 2: The discrete part of the observed fluorescence spectrum of molecular oxygen (figure 1), i.e. the part of the spectrum at highest energies.

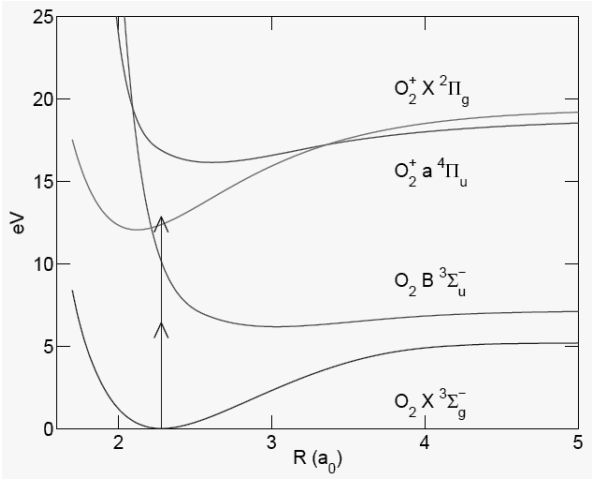

Figure 3: The potential energy curves that are relevant for the current problem. For O_2 the potential energy curves of the $X^3\Sigma_g^-$ and $B^3\Sigma_u^-$ states are shown and for O_2^+ those of the $X^2\Pi_g$ and $a^4\Pi_u$ states are shown. Also a two-photon excitation from the ground state is drawn as two arrows.

It appears from literature that this spectrum has been observed previously a few times.[2, 3] The authors of these articles speculate that it may belong to a state that is O_2^+-like, but without a definite assignment. More recently Bominaar [4] has suggested that the upper state involved might be the lowest member of the Rydberg series converging to the $A^2\Pi_g$ state in O_2^+. For the lowest state involved in the process he suggested the well-known $B^3\Sigma_u^-$ state, at least for parts of the spectrum. It is this latter suggestion that has been tested in this study.

The fluorescence spectrum is quite unusual. For an emission or fluorescence spectrum, one would expect to see relatively broad peaks because of rotational redistribution in the intermediate and final state. It is also expected that the peaks come closer together with decreasing energy until a certain energy, the dissociation limit of the final state. This is expected since vibrational levels come closer together, when they are closer to the dissociation limit. Also, an emission or fluorescence spectrum usually contains between one and three very broad peaks at lower energies. In the measured spectrum the distance between peaks in the spectrum indeed decreases with increasing wavelength at high energies (approximately $\lambda < 215$ nm), but at lower energies (approximately $\lambda > 215$ nm) many peaks can be seen with increasing distance. There is also a peak-broadening visible in the lower energy part of the spectrum. This strange behaviour has only been seen before for the NaK molecule.[5–7] The observed spectrum also shows peaks that are relatively narrow. This might be the result of predissociation of the higher energy state or of the fact that the spectrum is measured at "zero pressure". Both effects reduce the chance of a rotational redistribution and therefore reduce the rotational line broadening. The measurement at "zero pressure" also enlarges the lifetime of the intermediate state which, by the Heisenberg uncertainty principle, reduces the uncertainty in the measured energy. The predissociation on the other hand shortens lifetimes, which would mean a line broadening.

In this paper the upper state and final state of the fluorescence process will be determined. For the upper state the assumption is made that it is a Rydberg state. As will turn out later, by drawing molecular orbital diagrams, it indeed is a Rydberg state with as core the ionic $a^4\Pi_u$ state. The final state will be determined from its dissociation limit as derived from the measured spectrum. Also an assignment of the peaks in the discrete part of the measured spectrum will be given, together with calculated relative intensities.

II. THEORY

To obtain the measured fluorescence spectrum, a laser with a wavelength of 193.4 nm has been used. The fact that the laser needs to be focused in order to obtain the spectrum implies that a multi-photon absorption takes place. In this study the assumption has been made that the occuring transition is a two-photon absorption, although absorption of more photons can't be ruled out. For this reason the excitation energy of a two-photon excitation from the ground state has been drawn as arrows in figure 3. As has been noticed before, the initial state of the process is the vibrational ground state, $X^3\Sigma_u^-(v = 0)$ of neutral oxygen, O_2. Upon absorbing multiple photons, the molecular oxygen gets excited to an unknown state. After that, it falls back in energy, whilst emitting a fluorescence photon. The final energy state that is reached, is also unknown.

Since the initial energy state (ground state oxygen with $v'' = 0$; the rotational quantum number is unknown) is well-known and the energy of the absorbed photons is well-defined, the exact energy level of the intermediate state can be calculated, even though the exact vibrational level is unknown. From this single vibrational energy level of the intermediate state, fluorescence occurs to the vibrational levels of the final state. Because the spectrum is measured at room temperature, the measurements are not accurate up to rotational level. The population of the initial state will follow a Boltzmann distribution over rotational levels. This is expected to limit the rotational energy of the initial state to a range of the order of kT, which will broaden the peaks in the spectrum. The fluorescence peaks of the spectrum will have a P-branch and an R-branch that reflect the rotational distribution. This may account for the forked structure of some of the measured peaks. In the calculations that are made, the rotational effect will be neglected.

For known potential energy curves as function of the internuclear distance, eigenvalues (i.e. vibrational energies) ϵ and eigenfunctions $\chi(R)$ of the Hamiltonian operator were approximated by using a Discrete Variable Representation (DVR) method as mentioned in [8]. For this method, a grid has been chosen for the R-axis with a grid spacing of Δ. For a certain grid spacing, the set $\left\{\phi_n = \frac{1}{\sqrt{\Delta}}\mathrm{sinc}\left[\pi(\frac{x}{\Delta} - n)\right] \text{ with } n \in \mathbb{Z}\right\}$ has been taken as basis, where $\mathrm{sinc}(x) := \frac{\sin(x)}{x}$. This choice of a basis set has the nice property that any wavefunction $\psi = \sum_n c_n \phi_n$ at the n^{th} gridpoint takes as value the coefficient c_n of the basis function ϕ_n divided by $\sqrt{\Delta}$. Therefore the set of basis functions can be truncated at n equal to the size of the grid for R.

To determine the probability of occurrence of a transition between different energy states, one has to calculate the transition intensities. If a transition intensity is higher, the transition is more likely to occur. To calculate the transition intensity for overlap between an initial state $\psi^i_{v''}$ and a final state $\psi^f_{v'}$, one has to determine the squares of the matrix elements of the transition dipole

$$\mu_{fi} = \langle \psi^f_{v'} | \psi^i_{v''} \rangle. \tag{1}$$

The lables i and f denote the initial and final electronic states and the labels v denote the vibrational states. In the Born-Oppenheimer approximation $\psi^f_{v'} = \phi^f(\underline{q}; R)\chi^f_{v'}(R)$ with $\underline{q}$ the electronical coordinates and similar for the initial state. The equation then reduces to

$$\mu_{fi} = \int (\chi^f_{v'}(R))^* \mu(R) \chi^i_{v''}(R) dR, \tag{2}$$

where $\mu(R)$ is an integral over $\underline{q}$. Since for the present case nothing is known about its R-dependence, $\mu(R) = 1$ has been taken in this study. This reduces the expression to $|\int \chi^*_f(R)\chi_i(R)dR|^2$. Within these approximations, the transition intensities are called Franck-Condon factors, or simply FC-factors.

In any numerical (and therefore discrete) representation, the integral in the expression for FC-factors can be replaced by a summation over all gridpoints according to $\int \chi^*_f(R)\chi_i(R)dR \approx \sum_k \chi^*_f(R_k)\chi_i(R_k)$, where R_k are the values for internuclear distance that lie on the chosen grid. In the specific discrete variable representation using sinc-functions, the wavefunction in all gridpoints is equal to the coefficient of the corresponding basis function divided by $\sqrt{\Delta}$, so if a wavefunction is written as linear combination of basis functions $\chi(R) = \sum c_i \phi_i(R)$ then $\chi(R_k) = \frac{c_k}{\sqrt{\Delta}}$.

Using this in the expression for the FC-factors gives

$$FC_{ij} = \left|\Delta \sum_k \chi^*_f(R_k)\chi_i(R_k)\right|^2 = \left|\Delta \sum_k \frac{c^f_k}{\sqrt{\Delta}} \times \frac{c^i_k}{\sqrt{\Delta}}\right|^2 = |\overrightarrow{c_f} \cdot \overrightarrow{c_i}|^2, \tag{3}$$

where $\overrightarrow{c_k}$ denote the vectors with coefficients of the sinc-functions used as basis in the DVR. The approximation that $\mu(R) = 1$ and the DVR combined therefore reduce the integral to an inner product of two vectors.

This gives an explanation as to why a continuum spectrum exists at all. As shown in figure 4a, there exist eigenfunctions of the Hamiltonian operator in the continuum that can be approximated by so-called *continuum wavefunctions*. Since transition strength is governed by the Franck-Condor factors, the existence of continuum wavefunctions allows transitions to take place from a bound state to a continuum state. Even though it usually gives very little structure, this effect can yield a spectrum with several peaks with varying width, as shown in figure 4b, depending on the relative position of the potential energy curves. Therefore the part of the measured spectrum for approximately $\lambda > 215$ nm most probably is a continuum spectrum.

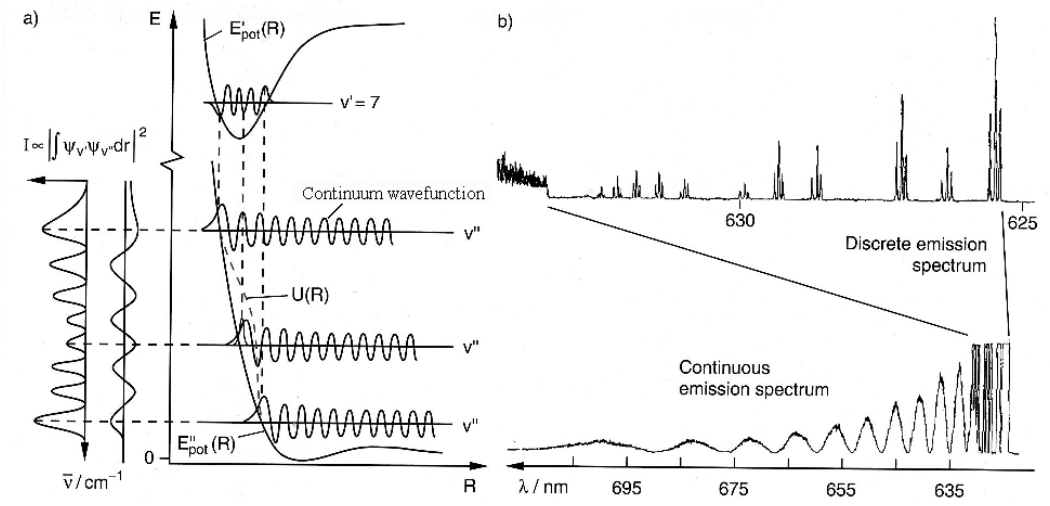

Figure 4: a) There exist eigenfunctions of the Hamiltonian operator that have an energy outside the bound states of the potential energy well. b) These states can yield a continuum spectrum which has several peaks with varying width and a distance that increases with the wavelength λ. The figure has been adapted without permission from [9].

It is essential for understanding the fluorescence spectrum to determine possible candidates for the intermediate and final state. To determine the final state, the energy corresponding to the borderline between the discrete and continuum parts of the spectrum, $\lambda = 215$ nm, can be used. This energy can be subtracted from the two-photon energy of $\frac{2 \cdot 10^7}{193.4}$ cm^{-1} (under assumption that a two-photon process takes place) which gives the approximate energy of the dissociation limit of the final energy state, $D_e = 7.05$ eV. There is only one bound state of oxygen having this dissociation energy, which is the $B^3\Sigma_u^-$ state. Therefore this must be the final state, if indeed two photons are absorbed by oxygen.

The intermediate state of the process is a lot more difficult to determine. This intermediate state has to be a bound state, since the excitation spectrum consists of sharp lines. (N.Dam, personal communication) To determine this state, molecular orbital diagrams with the appropriate electron configurations have been drawn for the initial and final states. They are shown in figure 5. For illustrative purposes, the spins in the text are treated similar to those in the figure. From the known electron configurations, the electron configuration of the intermediate state has been determined. Since the spectrum is observed in emission, the energy of the intermediate state has to be higher than that of the initial and final states. On the basis of transition strength the assumption will be made that single-electron transitions take place. The difference between the initial and final state is an electron that goes from the $1\pi_u$ to the $1\pi_g$ orbital. Since the unpaired electron in the π_u orbital of the final state has spin up, the excited electron must have spin down. It might also be that an electron with spin up gets excited, but then two electrons would have to do a spin-flip to arrive at the final state configuration, which would be very improbable. This gives an intermediate state in which one electron is highly excited, which makes it possible to consider the intermediate as an effective ionic state together with a single electron, and therefore as an ionic state which is slightly lowered in energy.

As can be seen in figure 5, the effective ionic state has three unpaired electrons with the same spin and it is therefore a quartet state. For the excited electron the only possible orbital we could think of, is a π_u orbital. There is only one quartet state of O_2^+ with an energy that's close to the energy of the assumed two-photon transition, which is the $a^4\Pi_u$ state. All other quartet states of the electron are either repulsive or have an energy that cannot be reached with less than 3 photons.

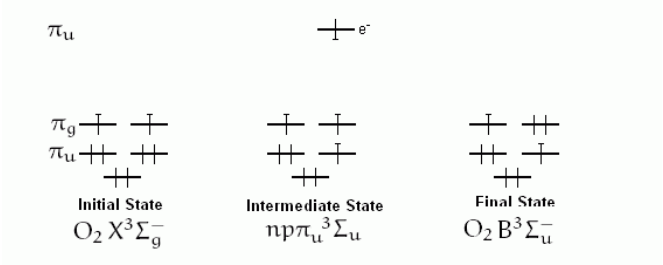

Figure 5: The only way in which an electron can go from a π_u to a π_g molecular orbital in a multi-photon process, is through a Rydberg state with a quartet ionic core. Therefore the only possible pathway for the fluorescence process from initial ground state oxygen to the $B^3\Sigma_u^-$ final state, is through a Rydberg state with an O_2^+ $a^4\Pi_u$ ionic core.

Because in the intermediate state one electron is highly excited, this electron feels the rest of the molecule effectively like a point charge of $+e$. (in atomic units a point charge of $+1$) Therefore this electron can be considered as a hydrogen-like electron. The states of a molecule in which one electron behaves roughly like a hydrogen electron are called Rydberg states. As it is with hydrogen, the energy of these hydrogen-like electrons rises with rising quantum number n, converging to an ionisation limit. The collection of such states with all principal quantum numbers n is called a Rydberg series converging to a particular ion state. In the case of molecular oxygen, the principal quantum number n has to be bigger than 2, because otherwise the electron would still be a valence electron. Also, the ionisation limit for this series is the potential energy curve of the ionic $a^4\Pi_u$ state, since at this stage, the electron is 'infinitely far away'. To describe Rydberg-series, the Rydberg formula is often used:

$$E_n = E_\infty - \frac{R_O}{(n-\delta)^2}. \tag{4}$$

In this formula E_n and E_∞ are the dissociation energy of the ion and of the Rydberg state, respectively. The third term in this equation is the energy difference between the Rydberg-state and the ion. R_O is the Rydberg constant for oxygen, which is $\frac{1}{2}$ in atomic units. Also a parameter δ is introduced in this formula. Since the electron is only hydrogen-like and not exactly a hydrogen electron, it would not be right to just have n^2 in the denominator of that fraction. This δ, which in fact is a first-order correction on the energy, is therefore called the quantum defect.

Since the energy of the intermediate state is well-known, whereas the quantum numbers of the level itself are unknown, the quantum defect is unknown. Once the vibrational level of the intermediate state is known, as well as its energy (calculated with the sinc-DVR method), the quantum defect can easily be obtained by rewriting the Rydberg-formula:

$$\delta = n - \sqrt{\frac{R_O}{E_\infty - E_n}} = n - \sqrt{\frac{R_O}{E^a_{v'} - E_{2f,gs}}}. \tag{5}$$

As has been said before, E_∞ and E_n are the energy levels of the dissociation limits of the ion and of the Rydberg level. Since the form of the potential energy well under the Rydberg assumption is the same for both the Rydberg state and the ionic state, the energy difference between the dissociation limits is the same as the energy gap between corresponding vibrational levels of the ion and the Rydberg level, in particular between the for the current problem relevant vibrational levels. Therefore $E_\infty - E_n = E^a_{v'} - E_{2f,gs}$, where $E^a_{v'}$ is the energy of the relevant vibrational level of the intermediate a state and $E_{2f,gs}$ is the sum of the energy of two photons of the used wavelength and the energy of the initial ground state. This last energy is equal to the energy of the relevant vibrational level of the Rydberg state.

III. SIMULATIONS

A. Potential energy curves

The potential energy curves of the $X^3\Sigma_g^-$ state of neutral oxygen and of the $a^4\Pi_u$ state of O_2^+ have been derived with a RKR method as described in [10] using spectroscopic data from [1]. With this method, one obtains a numerically determined formula $V(R)$ for the potential energy as function of internuclear distance. The input of an RKR-method

consists of vibrational term values and rotational constants. The formula is represented by the different vibrational energy levels (quantum number $v = 0, 1, \ldots$ with $v \in \mathbb{N}$) of the molecule that lie below the dissociation energy and the classical turning points corresponding to these energy levels. The derived formula only holds for the internuclear distances R between the classical turning punts of the highest vibrational state. For other internuclear distances, the potential energy values become less certain. When data are available for more vibrational energy levels, the result of this method is more accurate.

For the $a^4\Pi_u$ state of the ion the extrapolation for great internuclear distances of the potential energy curve resulting from the RKR method was not correct, since the dissociation limits of the ionic ground state and this state were around 3 eV apart, whereas according to [11] they should be the same. For the initial extrapolation an exponantial of the form $A\left(1-Be^{-\alpha x}\right)$ has been fitted such that the resulting function was continous on its entire domain and could be differentiated twice. To solve the problem an exponential of the same general form (i.e. $A'\left(1-B'e^{-\alpha' x}\right)$) has been fitted for nuclear distances greater than the largest tabulated internuclear distance of $v = 7$ such that the dissociation limit is correct and the potential is both continuous and differentiable, although only once, on its entire domain.

The potential energy curve of the $B^3\Sigma_u^-$ state has been derived with an RKR method as well, using spectroscopic data from [12, 13]. This time data were available for vibrational levels up to $v = 17$. For the potential energy curve of the ground state $X^2\Pi_g$ of the ion a Morse potential, which is a potential of the form $V(R) = D_e\left(1 - e^{-a(R-r_e)}\right)^2 + V_0$ has been plotted, using the spectroscopical constants D_e, r_e and a from [11]. Data on the minima of the different potential wells have, where necessary, been taken from [1].

B. Peak positions

As has been mentioned previously, an approximate dissociation limit of the final state could easily be determined, since the two-photon energy is well-known. The only bound state with the resulting dissociation limit, and therefore the only possible final state of the fluorescence process, is the $B^3\Sigma_u^-$ state. Another check on this state as final state of the fluorescence process can be done by calculating all expected peak positions in the spectrum.

Vibrational energy levels were computed with the sinc-DVR method for the potential energy curve of this state. As a next step, the energy differences between the two-photon energy and the eigenenergies of the B-state have been calculated to determine the theoretical peak positions in the spectrum. These calculated peak positions are shown in figure 6, together with the spectrum. Some of the calculated peaks (those with lowest vibrational quantum number v) fall in the region of the spectrum with a wavelength lower than 195 nm (which is the region with the highest energies), but these peaks are not shown in this figure. Peaks with these energies aren't measured, since the region is experimentally inaccessible.

In the figure, one can see that the positions of the two peaks at the high energy side of the measured spectrum (the peaks with wavelengths approximately 51080 cm^{-1} and 50500 cm^{-1}) coincide well with the calculated peak positions. Upon going to lower energies, the calculated peak positions become less accurate. This is probably due to residual error in the potential energy curve. Since an RKR-method has been used to obtain the potential energy curve, there is some error in the extrapolation for great internuclear distances R. In the case of the $B^3\Sigma_u^-$ state, however, this error should not be very large, since data are available for $0 \leqslant v''' \leqslant 17$. The effect of this error in the potential well seems to be a little stretching of the spacing between different energy levels. If the entire spectrum would be compressed from the low energy side, almost all calculated peaks would coincide with measured peaks. Since the peak spacing becomes smaller for peaks closer to the dissociation limit, these peaks will merge together a bit in the measured spectrum with respect to the calculated spectrum. This accounts for the peaks at a wavenumber of about 46800 cm^{-1}. Another point of interest is the fact that the calculated peak in the spectrum at a position of about 47570 cm^{-1} does not show up in the measured spectrum.

In the measured spectrum the peaks centered at a postition around 48700 cm^{-1} all have a smaller side-peak. The calculated spectrum does not account for those peaks and an explanation needs still to be sought for them. The bad correspondence of the third peak from the high energy side can be explained by the fact that a Raman peak of O_2 shows up at 50150 cm^{-1} [14]. This peak overlaps with the peak of the spectrum at the calculated position, which explains the strange observed form as well.

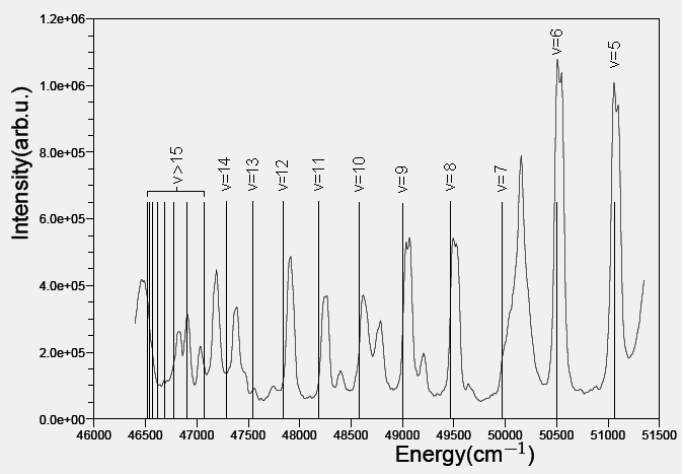

Figure 6: The discrete part of the measured spectrum, as well as the calculated peak positions. These calculated positions are the energies corresponding to the difference between the two-photon energy and the calculated energies of the vibrational levels of the $B^3\Sigma_u^-$ state.

C. Determination intermediate level

The next simulation that has been made is one of the FC-factors for overlap between the ground state X of oxygen and the previously determined upper state of the process, a Rydberg state of the $O_2^+ a^4\Pi_u$ state. To do this, the sinc-DVR method has been used on the potential energy curves of both states. Since the only difference between the potential energy curve of the Rydberg series and that of its ionic core under current approximations is a constant energy offset, the form of these potential energy curves is the same and therefore the wavefunctions of the Rydberg state and the ionic state are the same. For this reason the potential energy curve of the $O_2^+ a^4\Pi_u$ state has been used to obtain wavefunctions for the intermediate state.

The FC-factors have been calculated between the $v'' = 0$ level of the ground state of oxygen and the $0 \leqslant v' \leqslant 50$ states of the ion according to (1). A plot of the calculated FC-factors is shown in figure 7. For high vibrational quantum numbers, the results of this calculation do not have any physical meaning, since the corresponding vibrational levels would have an energy that lies in the continuum part of the potential. Because the sum of all FC-factors for a complete basis set needs to be 1 this still shows that most overlap between the ground state of oxygen and the a state of O_2^+ lies in the discrete part of the ionic state. Keep in mind that this figure is in fact a stick spectrum since $v \in \mathbb{N}$, although it is displayed otherwise.

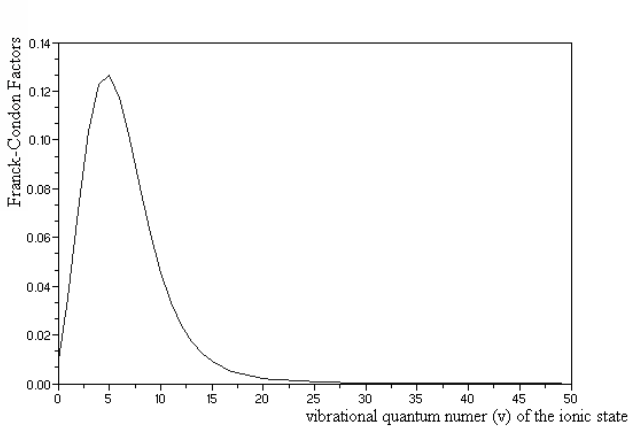

Figure 7: A plot of the calculated Franck-Condon factors for $O_2 X^3\Sigma_g^-(v=0) \longrightarrow$ Rydberg state of $O_2^+ a^4\Pi_u(v)$ transitions. The vibrational levels of the ion are drawn along the x-axis.

It has arbitrarily been assumed that a transition that gives a fluorescence spectrum with intensities as strong as the ones measured requires a FC > 0.02 between the initial and the intermediate state. For the a state of the ion this condition holds for $1 \leqslant \nu' \leqslant 12$. Since for this transition the assumption $\mu = 1$ has been made, a few extra vibrational states have been taken into account. For all selected vibrational levels (i.e. $0 \leqslant \nu' \leqslant 14$) of the ionic a state, the relative intensities, FC-factors, for the fluorescence spectrum have been calculated with the same method as for the FC-factors between the ground-state and the intermediate state. Some of these simulated spectra are shown in figures 8, 9 and 11. In these figures, also the calculated relative intensities for peaks with an energy that falls outside the measured spectrum are shown.

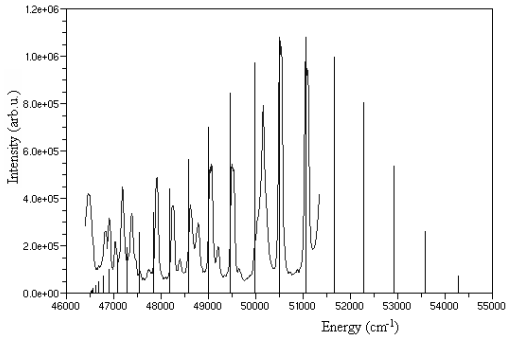

Figure 8: This stick spectrum shows the calculated relative intensities for transitions from the $\nu = 0$ state of the Rydberg level to the different vibrational levels of the final B state. The measured spectrum is shown as well.

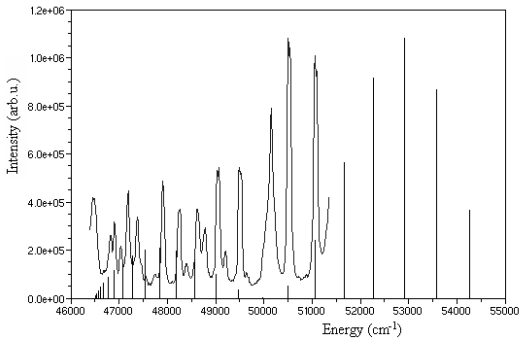

Figure 9: This stick spectrum shows the calculated relative intensities for transitions from the $\nu = 1$ state of the Rydberg level to the different vibrational levels of the final B state. The measured spectrum is shown as well.

In figures 8 and 9, the simulated relative fluorescence intensities are shown for the vibrational $\nu' = 0$ and $\nu' = 1$ intermediate levels. As can be seen, those spectra have less structure than the measured spectrum and therefore the upper state is not the $\nu' = 0$ or $\nu' = 1$ state. The spectra for a $\nu' = 0$ and $\nu' = 1$ upper state have an interesting property, though. They obey the reflection principle.[15, 16] This principle is illustrated in figure 10. It holds for a transition from a (low) vibrational level to a final state which is purely repulsive on the R-domain between the classical turning points of the initial state. If this condition holds, the spectrum of transition between these states, which is drawn along the vertical axis of the figure, is a mapping of the wavefunction of the initial state, as drawn at the horizontal axis of the figure.

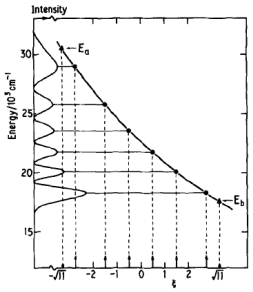

Figure 10: A schematic drawing of the reflection principle. The maxima of the measured spectrum (drawn on the vertical axis) correspond to the peak positions of the wavefunction on the horizontal axis. The figure has been reproduced without permission from [6].

This observation is in agreement with figure 3. The minimum of the potential energy well of the $B^3\Sigma_u$ state has an equilibrium distance that is higher than that of the $a^4\Pi_u$ state of the ion. It is therefore very well possible that the classical turning points of the lowest vibrational levels of the ionic state correspond to a purely repulsive part of the B state potential energy curve. The reflection principle shows for $\nu' = 0$ in figure 8, because the calculated spectrum has no nodes and the tops of the calculated peaks form the typical form of a ground state vibrational wavefunction. For $\nu' = 1$ in figure 9, there is exactly one node in the calculated spectrum, which agrees with a $\nu = 1$ vibrational wavefunction as well.

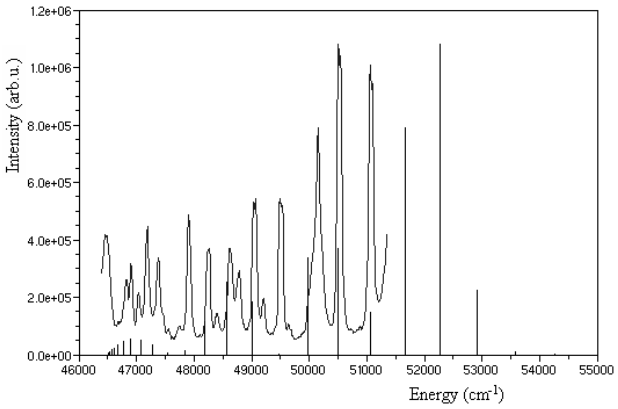

Figure 11: This stick spectrum shows the calculated relative intensities for transitions from the $v = 11$ state of the Rydberg level to the different vibrational levels of the final B state. The measured spectrum is shown as well.

In figure 11, the simulated spectrum is shown for the $v' = 11$ level of the $a^4\Pi_u$ state of the ion. The correspondence of the calculated relative intensities with the measured spectrum is reasonable. Contrary to all other calculated spectra with $v \geqslant 3$, the spectrum for $v' = 11$ shows some intensity for the peaks that lie close to the dissociation limits, which would allow the group of peaks around 47000 cm^{-1} in the measured spectrum to be visible.
The main points of concern in the simulated spectrum, are the apparent absence of peaks at 49500 cm^{-1} and 48000cm^{-1}, as well as the high predicted intensity of the peak that partly coincides with the previously mentioned Raman peak. This difference, as well as other smaller deviations from the measured spectrum, can be explained by the used approximation that $\mu = 1$, which is a very rough approximation. The uncertainty because of it as well as the bad correspondence of the other simulated spectra with the measured spectrum, enables one to say that a Rydberg state of the $O_2^+ a^4\Pi_u(v = 11)$ state is likely to be the upper state of the fluorescence process.

D. Quantum defect

Since the intermediate state is a Rydberg state of the $O_2^+ a^4\Pi_u$ state, most probably at $v' = 11$, the quantum defect δ is an important parameter. To determine the quantum defect, the energies of the different vibrational levels have been calculated. Since the energy of the Rydberg state is exactly known (the two-photon energy of the laser), the quantum defect can be determined according to (3) by the energy difference between the two-photon energy and the energy of the vibrational level. In table I some quantum defects are given for principal quantum numbers $n = 3$ and $n = 4$. As can been seen in this table, the quantum defect roughly varies between 1 and 2.5 for the given quantum numbers. In [17] a rule of thumb is given for quantum defects in atoms. According to this rule of thumb, quantum defects for a Rydberg electron in a p-state are in the order of magnitude of 0.75 for an *atom*. This rule of thumb does however say little about molecules. It still shows that quantum defects bigger than $\delta \geqslant 2$ are excessively high. Therefore the principal quantum number of the Rydberg-state is most probably $n = 3$. For the most probable vibrational level of $v' = 11$ this would give a quantum defect of $\delta = 1.281$.

$n = 3$		$n = 4$	
v'	δ	v'	δ
0	0.986	0	1.986
1	1.023	1	2.023
2	1.057	2	2.057
5	1.146	5	2.146
10	1.261	10	2.261
11	1.281	11	2.281
12	1.299	12	2.299

Table I: The calculated quantum defects δ for different principal quantum numbers n and vibrational levels v'.

IV. FUTURE RESEARCH

To fully understand the measured spectrum (fig.1) a lot of work still needs to be done. A first step that is necessary to take, is the determination of the transition dipole $\mu(R)$. As long as this function is unknown, the calculated Franck-Condon factors and relative intensities, will be inaccurate. If the transition dipole could be approximated by a numerical method on the same distance-grid that is used for the sinc-DVR method, it would already be an improvement.

Another step that is essential for solving this problem is the determination of more accurate potential energy curves. The potential energy curve that needs most attention, is that of the a state of the ion, since the only data available are data for vibrational levels $0 \leqslant v' \leqslant 7$. A first approach to obtain better potential energy curves, would be to get spectroscopical data about more vibrational levels. Upon knowing more data on vibrational levels a potential energy curve obtained by an RKR method will become more accurate. A different approach to obtain potential energy curves would be the use of an *ab initio* calculation.
If an *ab initio* calculation is done, the potential energy of the Rydberg state itself might be calculated as well. This would reduce the error of the current approximation that the potential energy curve of the Rydberg state is that of O_2^+ a- state lowered by a constant energy.

Since the spectrum has been measured at room temperature, there are different rotational levels occupied in the initial ground state oxygen. The occupation will follow a Boltzmann distribution. The fact that different rotational levels are involved influences the lineshape, mainly by broadening the peaks. It also results in an uncertainty of the intermediate level energy. In future work on the spectrum, this effect can be taken into account as well.

The major problem that still remains in the measured spectrum is the continuum part of it and the fact that it has so much structure. For this part of the spectrum, the involved states are unknown at this moment, although it is very likely that the upper state will be the same (Rydberg) state as in the discrete part of the spectrum. The final state might still be another state than the B state of neutral oxygen, although it would need to have the same dissociation limit. To calculate the spectrum once the involved states are determined, the renormalized Numerov method of [18, 19] can be used.

V. CONCLUSION

The fluorescence spectrum that is measured when a focused laser beam of 193.4 nm is absorbed by pure ground state molecular oxygen falls apart in two distinct regions, a discrete part for approximately $\lambda \leqslant 215$ nm and a continuum part for higher wavelengths and therefore for lower energies. In the discrete part of the spectrum, the final state of the occurring fluorescence process is the $B^3\Sigma_u^-$ state of neutral oxygen. The intermediate state of the process in the same region of the spectrum is very likely to be the Rydberg state of $O_2^+ a^4\Pi_u(v = 11)$ with principal quantum number $n = 3$. The FC-factor for the transition from the initial ground state is approximately $FC = 0.030$. The quantum defect for this Rydberg state is $\delta = 1.281$. The continuum part of the spectrum still needs to be explained.

[1] P. H. Krupenie, J. Phys. Chem. ref. data **1**, 423 (1972).
[2] G. Laufer, R. L. McKenzie, and W. M. Huo, Opt. Lett. **67**, 99 (1988).
[3] M. Versluis, Ph.D. thesis (1992).
[4] J. Bominaar, Ph.D. thesis (2008).
[5] D. Eisel, D. Zevgolis, and W.Demtroeder, J. Chem. Phys **71**, 1005 (1979).
[6] M. S. Child, H. Essén, and R. J. LeRoy, J. Chem. Phys **78**, 6732 (1993).
[7] R. J. LeRoy, W. J. Keogh, and M. S. Child, J. Chem. Phys **89**, 4564 (1988).
[8] G. C. Groenenboom and D. T. Colbert, J. Chem. Phys **99**, 9681 (1993).
[9] W. Demtroeder, *Atoms, Molecules and Photons* (2006).
[10] R. J. LeRoy, *Unpublished Report* (1991).
[11] D. L. Yeager, J. A. Nichols, and J. T. Golab, J. Chem. Phys **100**, 6514 (1994).
[12] A. S.-C. Cheung, K. Yoshino, W. H. Parkinson, and D. E. Freeman, J. Mol. Spectr **119**, 1 (1986).
[13] A. S.-C. Cheung, K. K.-W. Mok, Y. Sun, and D. E. Freeman, J. Mol. Spectr **163**, 9 (1994).
[14] A. C. Eckbreth, *Laser diagnostics for combustion temperature and species* (Abacus Press, 1988).

[15] R. Schinke, *Photodissociation Dynamics* (Cambridge University Press, 1993).
[16] M. G. Boogaarts, P. C. Hinnen, and G. Meijer, Chem. Phys. Lett **223**, 537 (1994).
[17] C. Y. R. Wu, L. C. Lee, and D. L. Judge, J. Chem. Phys **80**, 4682 (1984).
[18] B. R. Johnson, J. Chem. Phys **67**, 4086 (1977).
[19] B. R. Johnson, *The log derivative and renormalized numerov algorithms* (1977).